Computers in Biology and Medicine 39 (2009) 8 – 15

Contents lists available at ScienceDirect

Computers in Biology and Medicine

journal homepage: www.elsevier.com/locate/cbm

Heart sound reproduction based on neural network classification of cardiac valve disorders using wavelet transforms of PCG signals

Sepideh Babaei[a], Amir Geranmayeh[b,*]

[a]Department of Biomedical Engineering, Amirkabir University of Technology (Tehran Polytechnic), 15914 Tehran, Iran
[b]Department of Electrical Engineering and Information Technology, Darmstadt University of Technology, 64289 Darmstadt, Germany

ARTICLE INFO

Article history:
Received 15 September 2007
Accepted 20 October 2008

Keywords:
Cardiac auscultation
Heart valve disorders
Sound signals reproduction
Multiresolution analysis
Artificial neural network
Fast wavelet transform

ABSTRACT

Cardiac auscultatory proficiency of physicians is crucial for accurate diagnosis of many heart diseases. Plenty of diverse abnormal heart sounds with identical main specifications and different details representing the ambient noise are indispensably needed to train, assess and improve the skills of medical students in recognizing and distinguishing the primary symptoms of the cardiac diseases. This paper proposes a versatile multiresolution wavelet-based algorithm to first extract the main statistical characteristics of three well-known heart valve disorders, namely the aortic insufficiency, the aortic stenosis, and the pulmonary stenosis sounds as well as the normal ones. An artificial neural network (ANN) and statistical classifier are then applied alternatively to choose proper exclusive features. Both classification approaches suggest using Daubechies wavelet filter with four vanishing moments within five decomposition levels for the most prominent distinction of the diseases. The proffered ANN is a multilayer perceptron structure with one hidden layer trained by a back-propagation algorithm (MLP–BP) and it elevates the percentage classification accuracy to 94.42. Ultimately, the corresponding main features are manipulated in wavelet domain so as to sequentially regenerate the individual counterparts of the underlying signals.

1. Introduction

Nowadays, cardiologists have access to diverse techniques such as electrocardiograms, chest X-rays, ultrasound imaging, Doppler techniques, angiography, and transesophageal echocardiograph, to better inspect and scrutinize the functionality of heart. A typical visit by a cardiologist involving for instance ultrasound workup, however, is pretty expensive. Nonetheless, numerous studies have shown that considerably high percentages, i.e., even as much as about 87 percent of those referred to the cardiologists do not have any serious problems [1] and of course, the present situation is not what efficient medical care is all about.

The old-aged art of the heart sound analysis is yet widely exploited as a non-invasive technique to primarily examine the functionality of heart and in some circumstances auscultation might be the only possible approach available in hands of physicians. Heart sounds, traditionally heard through a stethoscope, are generated when the event of opening or closing of valves occurs in the heart. The sound normally comprises of four intermittent parts, among which the two dominant components caused by the valves closing, known as the first heart sound (S1) and the second heart sound (S2), are clearly audible, Fig. 1. The third heart sound (S3) is caused right after S2 by vibration of the ventricular walls, resulting from the first rapid filling, and the fourth (S4) occurs during the second phase of ventricular filling just before S1 when the atriums contract.

Aberrations and murmurs caused by the defective functionality of the valves, however, may also contribute in generation of these sounds [1,2]. Hence, physicians should be able to diagnose any kinds of such abnormalities throughout hearing the heart sound on the four locations commonly recommended for heart auscultation, Fig. 2 [2]. The low-pitched S1 is best heard in the mitral area since it is caused by the closure of the mitral and tricuspid valves. The louder but of shorter duration S2 is due to the closure of the pulmonary and aortic valves, and hence, that is best heard over the aortic area [2].

Accurate diagnosis via auscultation principally requires high qualification and extensive practical experience of the physicians [2]. Regardless of the wide availability and low-cost of auscultation diagnosis, however, internal medicine and family practice residents averagely recognize only 20% of all cardiac events and the number of correct identifications improves a little bit within years of inconsiderate training process [1]. In fact, due to the physical characteristics of the heart sound and limitations in human hearing capabilities [3],

* Corresponding author. Tel.: +49 6151 164661; fax: +49 6151 164611.
E-mail addresses: s.babaei@bme.aut.ac.ir (S. Babaei), geranmayeh@temf.tu-darmstadt.de (A. Geranmayeh).

0010-4825/$ - see front matter © 2008 Elsevier Ltd. All rights reserved.
doi:10.1016/j.compbiomed.2008.10.004

it may take several years for practitioners to fully acquire the skill of cardiac diagnoses based on real heart sound hearing. Hence, various samples of disordered heart sounds with identical main characteristics and different details simulating the ambient stochastic noise and the breath sound are needed to enhance the teaching and evaluation of the generalists in the field of cardiac auscultation skills.

Pertinent to the transient nature of the heart sound signals, the traditional frequency-domain analysis is incapable of precise process of such sharply varying signals with abrupt frequency changes [4–6]. In other words, many important fine details of the local time events may be lost if the discreet Fourier transform analysis is employed. In recent years, the multiresolution analysis technique has been extensively invoked for the statistical pattern recognition as well as proper detection of the occurrence time of small-scales features [7–9]. Owing to the highly time-varying nature of the stationary heart sound signals, the multiresolution analysis framework is a promising candidate to explore the dominant features and hidden information of the recorded clinical data simultaneously in time and frequency domains. Hence, the multiresolution context of the wavelet transform makes it a well-suited choice for the heart sound analysis [10–13]. In fact, wavelet transform optimally provides time-varying monitoring-window sizes, being adjustable wide for slow frequencies and narrow enough to track rapidly changing ranges [3]. Taking advantages of wavelet capabilities, variety of intelligent systems have been developed to classify types of heart sound abnormalities for symptom detection and machine-aided diagnosis [13,14], where mostly the wavelet transforms have been only applied for segmentation and feature extraction in conjunction with neural networks for classification of the graphic record of heart sounds, phonocardiogram (PCG) signals [4,15,16]. Machine learning methods have been mostly limited to diagnosing systolic and diastolic murmurs [17]. Nevertheless, a comprehensive automatic diagnosis has not yet been performed in any of the aforementioned studies for general clinical practices [18]. This has been due to the strict dependency of the accuracy of the resulting diagnosis to the data acquisition method and patients conditions, besides many practical difficulties in obtaining high-quality recordings with correct segmentation as well as infeasibility in the hardware level owing to the high execution time demand and memory requirements of the proposed algorithms [19]. All in all, disability in appropriate diagnosis of all types of cardiac disorders detected by the heart sound is yet a considerable challenging issue [18–23].

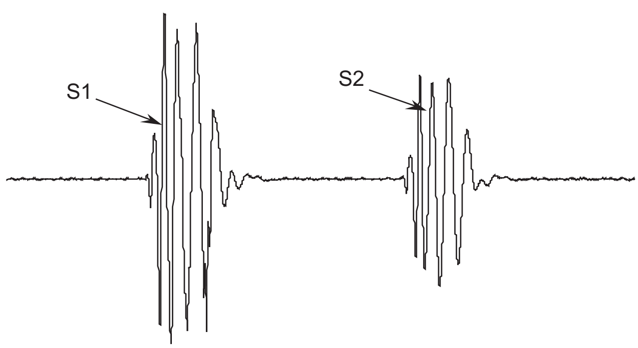

Fig. 1. Phonocardiogram (PCG) of a normal heart in a cardiac cycle.

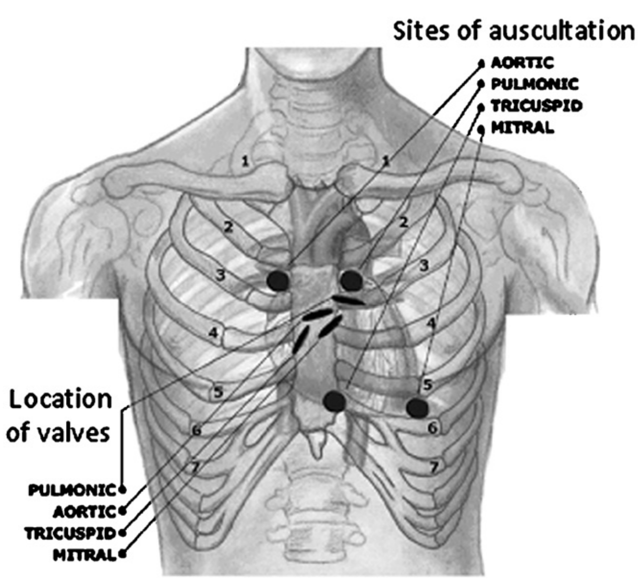

Fig. 2. Locations of heart auscultation [2].

This study aims to primarily aid physicians in practicing the art of auscultation by generating various heart sounds in desired cycles rather to supersede their expertise in auscultation and final judgment. To this end, the present work first investigates feature extraction of the most frequently needed sorts of the PCG signals, namely the aortic stenosis (AS), the aortic insufficiency (AI), the pulmonary stenosis (PS), and the normal (NL) one, using the multiresolution wavelet decomposition technique. The best diagnosing features are extracted using an artificial neural network (ANN) classifier. Various time-variant heart sounds are then adaptively reproduced using the reconstruction of the synthesized data. The general procedure has been outlined in the schematic diagram, Fig. 3. The accuracy of the developed training system is verified and the practical implementation concerns are discussed as well.

2. Discrete wavelet transform (DWT)

The DWT has been extensively used in signal processing, coding, denoising, image compression, etc. [8]. The DWT departs a signal into approximation (A) and detail (D) counterparts using a pair of orthogonal quadratic mirror filter (QMF) blocks as depicted in Fig. 4. In the DWT, the input signal is initially decomposed into two equal-length synthesized sequences by passing throughout the low-pass and high-pass decomposition filters with the impulse responses of h_k and g_k, respectively, and then, down-sampling the outputs by the factor of two, i.e., discarding even samples of the data [6]. Considering the sound signal produced during each cardiac cycle as a vector a^0 in time-domain, the DWT is formulated by

$$a^{j+1}(n) = \sum_k h(2n-k)a^j(k) \tag{1}$$

$$d^{j+1}(n) = \sum_k g(2n-k)a^j(k) \tag{2}$$

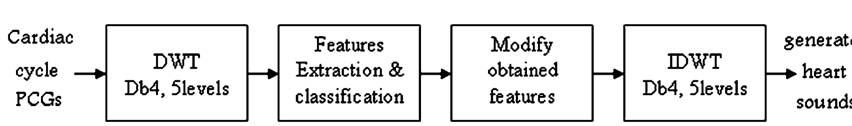

Fig. 3. The procedure of heart sound regeneration.

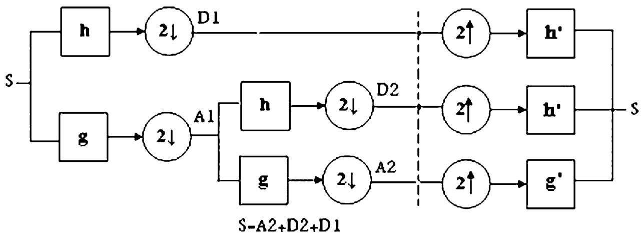

Fig. 4. The structure of the QMF bank for two resolution levels.

where the vector a^j at the resolution level j is decomposed into the smooth approximation part a^{j+1} and the finer detail part d^{j+1}. Continuing the process of recursive decomposition of the approximation vectors a^{j+1} for $j = 0, \ldots J-1$, one subsequently obtains the DWT of the vector a^0 at the resolution level J consisting of a^J, containing the coarsest approximation of the heart sound, and $d^j, j = 1, \ldots J$, possessing the local measure of the finer details. Conversely, the sequence a^j at stage j can be perfectly reconstructed from the two sequences a^{j+1} and d^{j+1} at any intermediate stage j+1, similarly using the two reconstruction quadrature filters coefficients h'_k (low-pass) and g'_k (high-pass). The reconstruction is, in principle, equivalent to first up-sampling the two corresponding sequences, i.e., inserting a zero between each two consecutive data samples, and then passing the resultant sequence through the two (bi)orthogonal reconstruction filters, and finally summing the two outputs up, i.e.,

$$a^j(n) = \sum_k h'(n-2k)a^{j+1}(k) + \sum_k g'(n-2k)d^{j+1}(k). \tag{3}$$

It is worth mentioning that the decomposition coefficients a^{j+1} and d^{j+1} obtained for various resolution levels actually describe the amount of correlation of the input signal with the dilated and shifted version of original basis waveforms, so called the scaling function and its complementary mother wavelet [8].

3. Data acquisition strategy

Valve-related heart diseases significantly affect the heart sound in a range that numerous cardiac abnormalities can be directly detected by careful auscultation. The first sound (S1) comprises of synchronous closure of the mitral and tricuspid valves in such a way that the two sounds merge to S1. When considered separately the closure of the mitral and tricuspid valves are called M1 and T1, respectively. The second sound (S2) is caused by the closure of the aortic and pulmonary valves. The pulmonary valve closure, so-called P2, happens slightly after the aortic component (A2). Generally, the frequency content of the sound S1 with two major energy-concentrated portions (corresponding to the M1 and T1) ranges between 10 and 180 Hz and the S2 spectrum extends from 50 to 250 Hz. Jointly, the frequency spectrum of normal PCG signals captures the interval 30 to 200 Hz [3], whereas the spectral components of the abnormal heart sounds may broaden around 10 Hz upto 700 Hz [17].

The stochastic sounds of the heart disorders were recorded on a multimedia personal computer equipped with an electronic stethoscope (Androscop IS28A00), sweeping the frequency range from 20 Hz to 20 kHz. Signals were digitized by a soundcard providing the sampling frequency of 11025 Hz with 16-bit resolution. Considering the frequency content of the heart sounds, this sampling rate provides a sufficiently high resolution for an in-depth analysis of every cycle apart from the rest [10,20]. The sounds were recorded on four locations of heart auscultation equivalently from male and female adult patients of Tehran Heart Center by averaging age of 35 years old. All patients had been examined with echocardiography by experienced cardiologists without using electrocardiogram. For exact record of the abnormalities, auscultation instructions such as the patient sitting position and the breathing phases (inspiration and expiration) are considered in each case. The AI murmur is early diastolic and best heard at the aortic area in the expiration phase when the patient sitting forward whereas the systolic murmur in AS is invariant with the respiration. In the PS, P2 is delayed and S2 splitting is accentuated during inspiration [2].

The sounds of most frequently affected disorders, namely the AS, AI, and PS, as well as the normal hearts were picked up for processing. Any of diseases affects individual cycles of the heart sound including {S4, S1, S2, S3} in a way that each cycle alone conveys the specifications of the underlying disease [2,10]. Therefore, the PCG signals were segmented into 372 sample segments, each involving a single cardiac cycle including 102 cycles belong to the normal group and 96, 92, 82 cycles, respectively, for AI, AS, PS cases. The gathered signals were divided into two packages, one including 234 cycles for feature extraction of the four categorized groups of AS, PS, AI disorders, as well as the normal sound (each group consisting 60 cycles for AS, AI, normal training and 54 cycles for PS training), and the other package preparing 138 cycles for testing the accuracy of classification routine.

4. Feature extraction

The fast Fourier transform (FFT) analysis of S2 cannot specify the time delay splitting A2 and P2 [23], or which one precedes the other [9], that are of essential importance in identification of pathological cases [2]. Hence, wavelet transformations are proffered to extract the particular features of the heart sound abnormalities. Several orthogonal wavelets are exploited here to decompose the prepared heart sound signals into different resolution levels using the fast wavelet transform described in Section 2. The detail coefficients of every resolution level and the approximation coefficients of the last decomposition level are utilized to determine a feature vector (FV) for any recorded samples belonging to each one of the four categorized groups, consisting of the three disorders and normal heart sounds. The FV is supposed to represent statistical characteristics of the DWT coefficients so that one can conveniently classify the synthesized data. Each signal group can be conceived as a cluster for which the center and spread of its wavelet coefficients are gauged by the mean and standard deviation (STD) operators, respectively. The mean value infers the statistical averaging (frequency content around the origin) of the wavelet coefficients and the STD measures the scatter of different trials from the mean value. Hence, the first FV element is defined as the mean value of the approximate coefficients of the decomposed signals at the deepest decomposition level and the second entry is filled by the STD of the approximation coefficients at the last level. Consequently, all other entries are completed by the mean value and STD of the detailed coefficients obtained for every octave levels. The FVs with length $M = 2J$+2 are constructed for all P training samples. Ultimately for the reproduction, the average of the two statistical characteristics (the mean value and the STD) of the P FVs with overall length M is designated to each group of the disorders.

4.1. Neural network classification

The ANN is a heuristic mathematical model involving number of highly interconnected processing layers inspired by human brain regime [24]. The ANN provides learning capabilities based on its natural propensities in storing and recursive usage of the experimental knowledge. By virtue of its parallel distribution, the ANN is generally robust, tolerant of faults and noise, able to well generalize and capable of solving non-linear problems [17].

A multilayer perceptron (MLP) neural network, as described in Fig. 5, is used for classification of three different cardiac disorders and normal heart sound. The FVs are used as the inputs to the network. The input layer, thus, consists of M nodes indicating the input features. The four categories of heart sounds are encoded according to the following binary assignment for the output layer:

$$\mathrm{AS} = [1, 0, 0, 0], \quad \mathrm{PS} = [0, 1, 0, 0], \quad \mathrm{AI} = [0, 0, 1, 0], \quad \mathrm{NL} = [0, 0, 0, 1].$$

After some preliminary simulations for the different network size with 12, 24, 48, and 96 hidden nodes, it turns out that 48 hidden nodes give the satisfactory performance. The architecture and parameters of the applied MLP network has been elucidated in Table 1. The network output vector is calculated by

$$Z_i = f\left(\sum_{h=1}^{49} W_{Y-Z}^{ih} f\left(\sum_{j=1}^{M} W_{X-Y}^{hj} X_j + \theta_1\right) + \theta_2\right) \tag{4}$$

where X is the network input vector with length M and W_{X-Y}^{hj} denotes the weight associated with the j-th unit of X to the h-th unit of the hidden layer vector Y with length 48. The coefficient W_{Y-Z}^{ih}

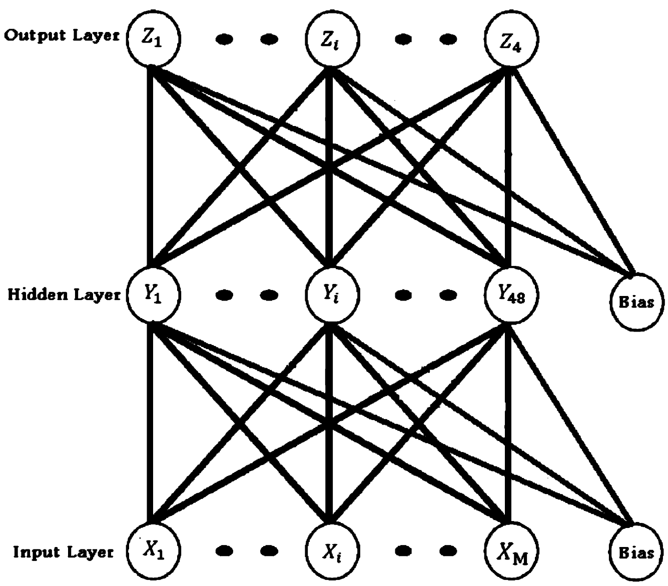

Fig. 5. The proposed MLP network with one hidden layer: The input layer has a bias node as well as M nodes indicating the length of the FVs as a function of decomposition levels; the hidden layer has 48 units plus a bias node and the output layer has four nodes denoting the class of the input data.

Table 1
The architecture and parameters of the designed MLP–BP network

ANN architecture:	
Number of hidden layer	1
Number of input units	*M*
Number of hidden units	48
Number of output units	4
Activation functions	Sigmoid
ANN training parameters:	
Learning rule	Back-propagation
Learning rate	0.1
Momentum term	0.7
Number of epochs	6000

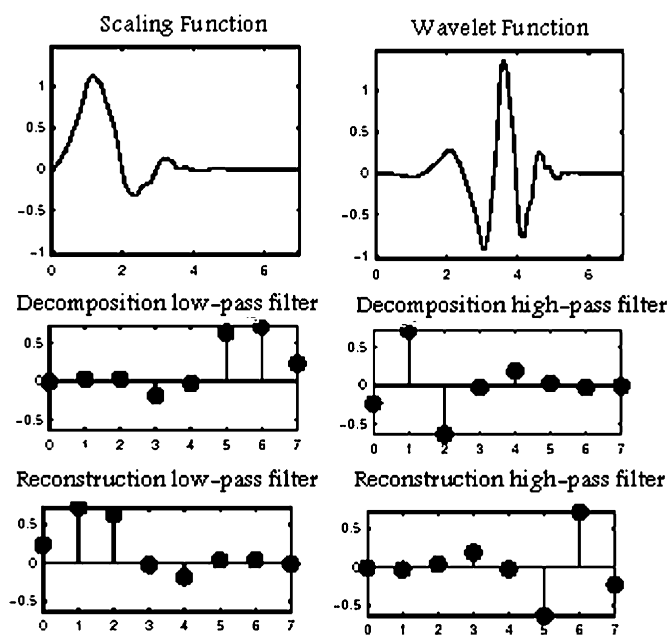

Fig. 6. Coefficients db4 analysis and synthesis filter bank.

Table 2
The percentage accuracy of the classification approaches using diverse wavelets in various decomposition levels for diagnosing heart valve disorders, (a) the neural network-based assignment and (b) the statistical classifier

Wavelet	Level									
	1	2	3	4	5	6	7	8	9	10
(a)										
db1 (Haar)	73.97	77.53	74.83	79.94	86.65	78.18	81.48	83.63	84.65	81.22
db4	60.36	57.93	75.18	89.51	**94.42**	85.18	89.39	90.55	89.65	82.59
coif3	52.12	42.39	70.23	86.82	83.42	85.33	81.59	83.23	81.91	82.84
sym5	55.41	50.37	68.87	88.24	90.77	85.78	84.43	86.55	89.17	81.96
rbio1.5	52.16	50.77	62.96	86.59	88.36	84.81	88.19	82.35	82.94	84.17
(b)										
db1 (Haar)	70.97	77.42	71.77	76.61	83.71	75.81	79.84	80.64	81.45	78.23
db4	52.42	46.77	70.97	87.1	**91.13**	83.06	88.87	87.1	87.1	81.45
coif3	53.23	46.77	66.13	84.68	89.52	83.87	79.84	82.26	79.84	79.84
sym5	50.81	46.77	66.13	84.68	88.71	83.87	83.87	84.68	87.1	83.06
rbio1.5	50.81	46.77	66.13	87.1	89.52	83.06	87.9	83.87	82.26	83.87

Feature extraction using the db4 decomposition filter within five resolution levels affords the best accuracy.

represents the connection weight between h-th unit of hidden layer and i-th unit of network output. The bias weights θ_1 and θ_2 are added to the neurons of the input and hidden layers, respectively. The input FVs classifies C_i if $Z_i > Z_j$ for all $j \neq i$, where $C_i = \{AS, PS, AI, NL\}$. The activation function (f) introduces nonlinearity into the network. For back-propagation (BP) learning, the activation function has to be differentiable. On the other hand, the stability of the feed-forward network, i.e., finite output, is guaranteed by the bounded functions. The logistic functions such as sigmoid, hyperbolic tangent, and Gaussian functions are the most common choices [25]. The sigmoid activation function $f = 1/(1 + e^{-x})$ provides an elegant compromise between linearity, nonlinearity, and saturation [25] and it bounds the neuron outputs between (0, 1).

The BP algorithm is applied to train the network using both a constant learning rate and a momentum term. Training is terminated when the upper limit of the training epochs is reached. When the training inputs are fed in a rhythmic pattern, the decreasing rate of the training error is imperceptible and the final error stands on 0.2. To avoid the local minima, the sequence of training inputs is reordered randomly at 1800th epoch. This causes the error to be lessened to the yet unsatisfactory level 0.16 after 6000 epochs. In order to enhance the performance of the intelligent system, random feeding strategy can be used during network training. When input samples are randomly rearranged for each epoch, the training error falls down to 0.05 within 6000 epochs.

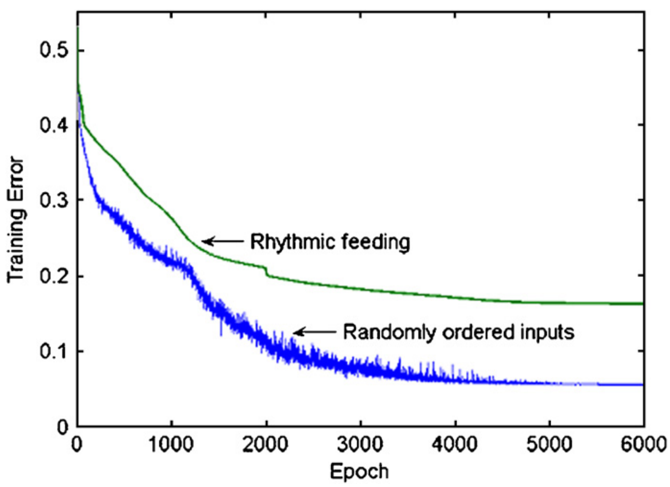

Fig. 7. The error of network training of the transformed feature vectors using db4 in five decomposition levels for 6000 epochs.

4.2. Statistical classification

Here the authors present an alternative approach for classification of cardiac diseases based on the statistical properties of the probed cycles similarly in the wavelet domain. For this purpose, almost half of the acquired signals are randomly exerted to extract the features of the three disorders and the normal groups, the remaining PCG signals are dedicated to examine the accuracy of the distinction based on the defined FVs. The latter are used to compute a set of test feature vectors (TV) similarly through decomposing the gathered test signals by the corresponding wavelet filters in equivalent resolution levels. For all case studies, the difference between the mean value of the FV and the TV is divided to the STD of the FV, i.e.,

$$b = \text{Ave}((\text{Mean}(FV) - TV)/\text{STD}(FV)) \tag{5}$$

where Ave( ) implies averaging over M samples of a vector. The final judgment is made based on the magnitude of the normalized distance between the two vectors FV and TV. Therefore, $b < 1$ assigns whether the signal belongs to the associated group or not.

4.3. Wavelet and resolution selection

The existing choices for the impulse response of the filters as well as decomposition levels alternatives may influence the precision of discriminating among the affiliated groups. The higher the correlation of the wavelet function and the normal PCG signal is, the more specifically an abnormality can be characterized, and thus, the more accurately it can be classified. Table 2 compares the classification performance of diverse suitable wavelets, mainly the

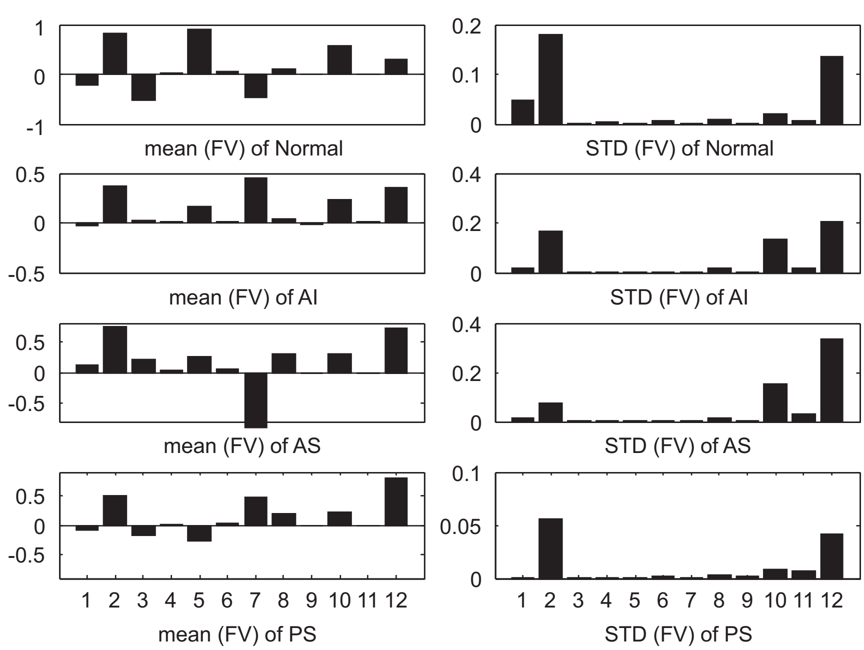

Fig. 8. Two characteristic vectors involving the mean value of the FV and the STD of the six resultant coefficients (D1, D2, D3, D4, D5, and A5), employed for reconstructing the heart sound signals of the four groups.

Haar, Daubechies with four vanishing moments (db4), third order Coifman (coif3), fifth order near symmetric Symlet (sym5), and reverse biorthogonal (rbio1.5) wavelets in 10 successive decomposition levels. It is worth noting that the coif3 has three vanishing moments in the scaling function and the rbio1.5 wavelet has five vanishing moments for the primal wavelet and linear smoothness for its dual wavelet [8]. The likelihood of success in diagnosing valve disorders through the ANN and the direct statistical classification approaches have been reported in Table 2 distinctively. It is observed that the experimental results obtained using the statistical classification fully comply with more precise outcomes of the neural network approach. It can be deduced from Table 2 that differences among the output judgments of the diverse wavelets are small, since the chosen wavelets shapes are relatively similar to the envelope of normal heart sounds [22]. Table 2 also discloses that the temporal and spectral differences between mentioned heart sounds are characterized and extracted more precisely by employing the db4 filters in comparison with the other wavelets. Therefore, the db4 wavelet transform, Fig. 6, is selected as the best choice and applied to the input signals in five decomposition levels.

Fig. 7 exhibits the error of network training pertinent to the FVs of the samples decomposed by the db4 within five resolution levels ($M = 12$) for 6000 epochs. The inspection of the results reveals 94.5 and 91.13% accuracy in exact dedication of the diseases to the relevant group for respectively the proposed ANN and the statistical classification methods. In this arrangement, on the next section, two characteristic vectors involving the mean value of the FV and the STD of the six resultant coefficients (D1, D2, D3, D4, D5, and A5), as sketched in Fig. 8, are employed to adaptively reconstruct the time-variant heart sound signals of the four groups. The tree diagram used for synthesis of the data is depicted in Fig. 9. Basically, the choice of the highest decomposition level $J = 5$ plays a significant role in improving the classification accuracy. As an example, diastolic murmurs in AI disease are obvious at fourth level of wavelet coefficients as observed in Fig. 10. Nevertheless, some useful information may vanish when one further proceeds in decomposition levels.

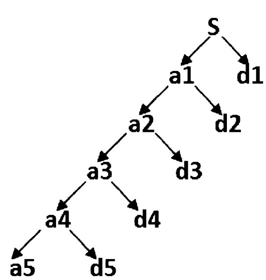

Fig. 9. The wavelet decomposition tree for the lowest resolution level $J = 5$.

5. Heart sound reproduction

As explained above, regardless of the classification type, one obtains an 1×12 array for each groups, including the mean value of the FVs as well as a real number indicating the mean of the STD of the corresponding FV. Using the extracted features to adaptively reproduce heart sound signals in desired cardiac time cycles for the AI, AS, PS disorders and normal heart was the main purpose of the discussed classification procedures. At this stage, the formerly evaluated FVs with $M = 12$ are randomly manipulated to produce numerous heart sound signals with the same main characteristics and differences on insignificant details in every cardiac cycle. The wavelet coefficients of the reproduced signals are supposed to be close to the wavelet coefficients of an original PCG with slight differences in statistical features, the mean and STD, Fig. 10. Thus, before the reconstruction phase is accomplished, a typical set of the evaluated wavelet coefficients are multiplied by normalized disturbance factors. The disturbance factors are obtained by adding the mean characteristic vector of the cluster with its corresponding STD characteristic vector multiplied by a randomly selected number in the range of $[-1, 1]$. These factors are normalized through division by the mean (approximate and details) coefficients of the typical chosen signal. Finally, the

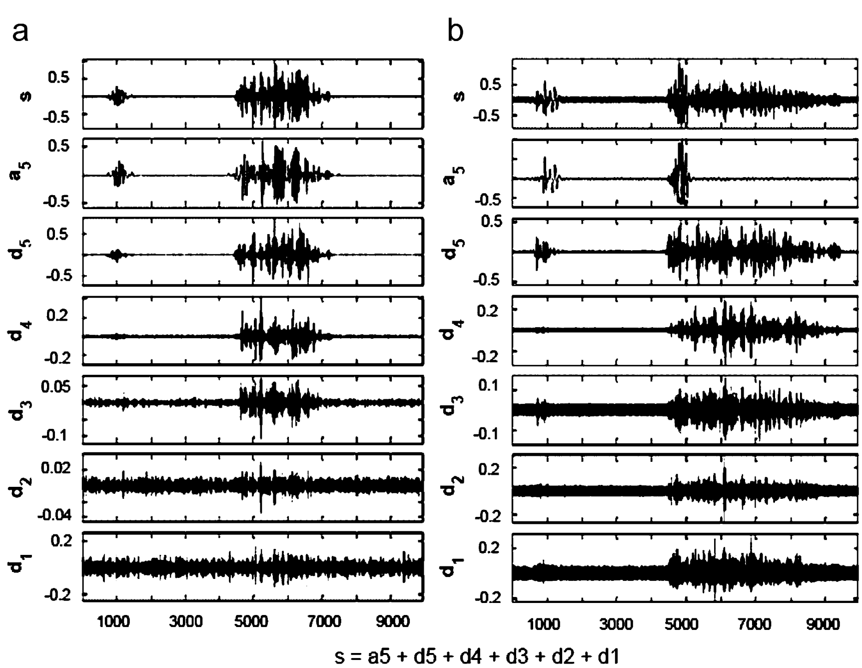

Fig. 10. Decomposition coefficients of a single cardiac cycle of AI PCG transformed by db4 up to five stages: (a) the original and, (b) the reproduced signal. The horizontal and vertical axes denote time and amplitude of coefficients, respectively.

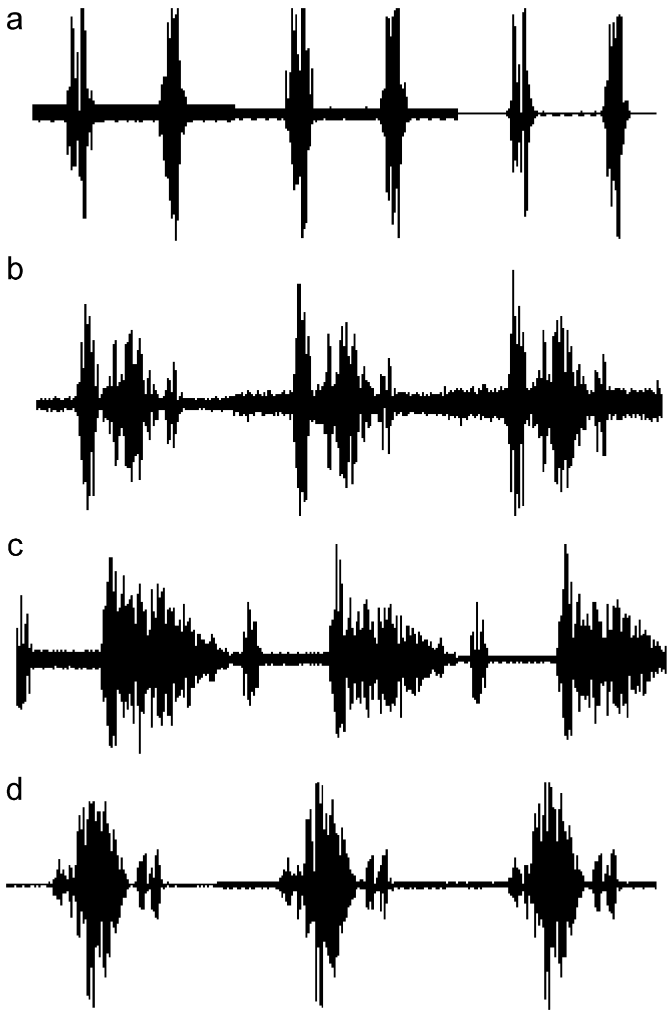

Fig. 11. The generated PCG signals for (a) a normal heart, and (b) AS, (c) AI, (d) PS disorders in three cycles.

updated five set of details and one set of approximation coefficients are accumulated for reconstruction of temporal samples by the inverse DWT.

Using the db4 synthesis filters, the reconstruction of the lately modified wavelet coefficients in the fifth resolution level is carried out to transfer the newly generated PCG signals form the wavelet-domain to the time-domain. This procedure can be readily continued for any number of desired cycles with arbitrary changes in coefficients that resides in the range of the STD of that specific group, i.e., only the six disturbance factors are automatically updated for generating every cycles. The PCG signals are saved on memory in the wave format, in separate files with "wav" extension. The real-time generation of cycles with random alternation is ready to be played one right after the other. All reproduced signals convey the special characteristics of the associated diseases, as displayed in Fig. 10. Spilt S2 in PS, systolic crescendo-decrescendo murmur in AS, diastolic decrescendo murmur in AI and normal S1 and S2 can be heard within the reproduced heart sounds vividly. As Fig. 11 clarifies, the inconsequential characteristics of the reproduced sounds are different in each cycle. The differences resemble the ambient noise and the patient breathing in realistic auscultation. Hence, listening to the reproduced heart sounds can more effectively improve the quality of the ear-training applications.

Table 3
Comparing five reproduced cycles of each group with the original clinical samples

Normal heart sound					
MED of FFT	0.0264	0.0273	0.0314	0.0422	0.1087
L2-norm difference	−0.01546	−0.26612	−0.11729	0.018132	0.058986
Time-domain MSE	4.26E−07	0.000105	2.40E−05	6.08E−07	6.72E−06
AI disorder					
MED of FFT	0.830	0.718	0.829	0.724	0.392
L2-norm difference	−0.90661	−0.44743	−2.2576	−0.35294	−0.87395
Time-domain MSE	0.000485	0.000128	0.002547	9.00E−05	0.000452
AS disorder					
MED of FFT	3.19	2.89	3.56	3.63	3.94
L2-norm difference	5.1042	4.7833	4.9469	4.8223	4.1953
Time domain MSE	0.10895	0.11042	0.10967	0.11024	0.11315
PS disorder					
MED of FFT	1.399	1.598	1.374	1.735	1.13
L2-norm difference	0.083959	−0.07876	−0.04791	0.060173	−0.24186
Time-domain MSE	0.061481	0.061954	0.061864	0.06155	0.062442

The comparison has been performed in three ways, namely the MED of the frequency spectrum (FFT), the differences of the Euclidian norms, and the MSE in time domain.

6. Verification of the produced signals

Identical main characteristics and different details in every cycle of the reproduced PCGs have been illustrated in Fig. 11. In order to more rigorously examine the accuracy of the introduced method, the frequency spectrums of the original and reproduced signals are compared. Evidently, the FFT of the original and reproduced samples do not exhibit any significant frequency differences that might be appeared in their associated sound signals and they have quit similar power spectrums distributions. The mean value of Euclidean distance (MED) of the FFT of the original and five cases of the reproduce sound have been tabulated in Table 3. Similarity of the signals in time domain may also be deduced by the small difference between the energy of the signals. Hence, the comparison is executed again, this time, however, by monitoring the difference between the norm-2 of five typical reproduced signals and that of the original test one, as set forth in the second rows of each category in Table 3. The presence of entries much smaller than one iterates conspicuous resemblance in the time evolution of the generated signals with the benchmarks.

Mean square error (MSE) indicating the goodness of fitness of the method, is another major criterion certifying the homogeneity of the general behavior of the regenerated signals,

$$MSE(x_1, x_2) = \left(\sqrt{\sum_{i=1}^{n} (x_{1i} - x_{2i})^2} \right) \Big/ n. \tag{6}$$

The extreme value of this index is 1.0, therefore, the MSE value of the outcome sequence much smaller than 1.0 also attest that the similarity of the original signal or its delayed version to the successively regenerated samples (their cross coloration) is sufficiently noticeable. As expressed in the last row of Table 3, the MSE values state admissible identifications between some successively reproduced signals and the original ones.

To experimentally validate how precisely the generated signals have been tabulated and to demonstrate the efficiency of the results in improving auscultation skills, the honesty of most serially generated signals was tested and confirmed by blind examination of the expert cardiologists in Tehran Heart Center.

7. Conclusion

Two effective types of classification strategies, the use of either neural network training or statistical averaging on an efficiently decomposed version of clinical samples, were proposed for separation of the heart valve abnormalities. The outcomes of the both classification approaches assert that the extracted features using the db4 wavelet transform in five resolution levels create acceptable distinctions among every pairs of the AS, PS, AI disorders and normal heart sounds. This can, furthermore, facilitate infinitely unique reconstruction of the modified wavelet coefficients without any group interference. Artificial counterparts of the original heart sounds were randomly regenerated by considerate manipulation of the wavelet coefficients. Cycles of the generated sound possess main characteristics in common with the underlying disease whereas they convey extrinsic differences in details simulating the ambient noise during the auscultation. This stochastic essence of the reproduce signals aids physicians to better perceive the key features of that particular disease in the presence of biological noises. The randomly regenerated heart sound signals can also be utilized to train and test medical students and interns so as to eventually promote the physical diagnostic skills in heart sound analysis art. The present algorithm also furnishes a feasible approach for non-stationary generation of signals for machine aided diagnosis of the heart disorders. The same methodology can be applied to simulate other heart diseases dynamically.

Conflict of interest statement

None declared.

Acknowledgment

The authors would like to thank the head of the education department of Tehran Heart Center, M.D. Mohebi, and the research consultant, M.D. Pishbin, for granting access to their facilities for recording heart sounds of patients and testing the reproducing technology.

References

[1] S. Mangione, L.Z. Nieman, Cardiac auscultatory skills of internal medicine and family practice trainees. A comparison of diagnostic proficiency, JAMA 278 (1997) 9.
[2] A. Tilkian, M. Conover, Understanding Heart Sounds and Murmurs, WB Saunders Co., San Diego, CA, 2001.
[3] P.M. Bentley, P.M. Grant, J.T.E. McDonnell, Time-frequency and time-scale techniques for the classification of native and bioprosthetic heart valve sounds, IEEE Trans. Biomed. Eng. 45 (1) (1998) 125–128.
[4] L.T. Halla, J.L. Maplea, J. Agzarianb, D. Abbotta, Sensor system for heart sound biomonitor, Microelectron. J. 31 (2000) 583–592.
[5] A. Mertins, Signal Analysis: Wavelets Filter Banks, Time Frequency Transforms and Application, Wiley, New York, 1999.
[6] M. Unser, T. Blu, Wavelet theory demystified, IEEE Trans. Signal Process. 51 (2) (2003) 470–483.
[7] B. El-Asir, L. Khadra, A.H. Al-Abbasi, M.M.J. Mohammed, Time-frequency analysis of heart sounds, IEEE TENCON—Digital Signal Process. Appl. 2 (1996) 553–558.
[8] T.K. Sarkar, C. Su, R. Adve, M. Salzar-Palma, L. Garcia-Castillo, R.R. Boix, A tutorial on wavelets from an electrical engineering perspective, part 1: discrete wavelet techniques, IEEE Trans. Antennas Propag. 40 (1998) 549–568.
[9] S.M. Debbal, F. Bereksi-Reguig, Automatic measure of the split in the second cardiac sound by using the wavelet transform technique, Comput. Biol. Med. 37 (3) (2007) 3269–3276.
[10] L. Huiying, L. Sakari, H. Iiro, A heart sounds segmentation algorithm using wavelets decomposition and reconstruction, in: Proceedings of the 19th Conference IEEE/EMBS, Chicago USA, vol. 4, 1997, pp. 1630–1633.
[11] Z. Telatar, O. Eroul, Heart sounds modification for the diagnosis of cardiac disorders, IJCI Proc Int. Conf. Signal Process. 100 (2) (2003) 105–111.
[12] T.R. Reed, N.E. Reed, P. Fritzson, The analysis of heart sounds for symptom detection and machine-aided diagnosis, in: Proceedings EUROSIM in Biology, Medicine and Biomedical Engineering, 2001, pp. 26–29.
[13] F. Rios-Gutiérrez, R. Alba-Flores, K. Ejaz, G. Nordehn, N. Andrisevic, Classification of four types of common murmurs using wavelets and a learning vector quantization network, International Joint Conference on Neural Networks, vol. 16 (21), 2006, pp. 2206–2213.
[14] N. Andrisevic, K. Ejaz, F. Rios-Gutierrez, R. Alba-Flores, Detection of heart murmurs using wavelet analysis and artificial neural networks, J. Biomed. Eng. 127 (6) (2005) 899–904.
[15] D. Kumar, P. Carvalho, M. Antunes, J. Henriques, M. Maldonado, R. Schmidt, J. Habetha, Wavelet transform and simplicity based heart murmur segmentation, Comput. Cardiol. 33 (2006) 173–176.
[16] E. Comaka, A. Arslana, I. Türkoglub, A decision support system based on support vector machines for diagnosis of the heart valve diseases, Comput. Biol. Med. 37 (1) (2007) 21–27.
[17] C. Navin Gupta, R. Palaniappan, S. Swaminathan, S. Krishnan, Neural network classification of homomorphic segmented heart sounds, Appl. Soft Comput. 7 (1) (2005) 286–297.
[18] A. Voss, A. Mix, T. Hubner, Diagnosing aortic valve stenosis by parameter extraction of heart sound signals, Ann. Biomed. Eng. 33 (9) (2005) 1167–1174.
[19] I. Turkoglua, A. Arslanb, E. Ilkayc, An intelligent system for diagnosis of the heart valve diseases with wavelet packet neural networks, Comput. Biol. Med. 33 (4) (2003) 319–331.
[20] M. Segaerl, O. Lilia, S. Lukkarinen, Computer-based detection and analysis of heart sound and murmur, Ann. Biomed. Eng. 33 (7) (2005) 937–942.
[21] P. Hult, T. Fjaellbrant, K. Hilden, U. Dahlstroem, B. Wranne, P. Ask, Detection of the third heart sound using a tailored wavelet approach: method verification, Med. Biol. Eng. Comput. 43 (2) (2005) 212–217.
[22] J. Tony, Heart sound analysis comparing wavelet and autoregressive techniques, Comput. Cardiol. (2003) 657–660.
[23] S.M. Debbal, F. Bereksi-Reguig, Computerized heart sounds analysis, Comput. Biol. Med. 38 (2) (2008) 263–280.
[24] S. Haykin, Neural Networks, A Comprehensive Foundation, Macmillan College Publishing Co., New York, 1996.
[25] F. Ham, I. Kostanic, Principles of Neural Networks for Science and Engineering, McGraw-Hill, New York, 2000 (Chapter 2).

Sepideh Babaei was born in 1981, in Tehran, Iran. She received the B.S. degree in Biomedical Engineering from Science and Research branch of Azad University, Tehran, in 2004 and the M.S. degree in Bioelectric from Department of Biomedical Engineering, Amirkabir University of Technology (Tehran Polytechnic) in 2008.
In 2003, she served as a hospital equipments technician of Rasoul-e Akram Medical Complex (RAMC), the educational hospital of Iran University of Medical Science. From 2004 to 2006, she was a research and service engineer in biotechnology and medical equipments in Tadjhiz-Gostar Co. (the exclusive representer of Eppendorf, Nikon, and NihonKohden companies in Iran). Her main research interests include intelligent systems, pattern recognition, and signal processing techniques, especially in bioinformatics.

Amir Geranmayeh was born in 1980, in Tehran, Iran. He received the B.S. degree in Electrical Engineering and M.S. degree (with distinction) in Telecommunication Engineering both from Amirkabir University of Technology (Tehran Polytechnic), in 2002 and 2005, respectively. Since 2005, he is a Ph.D. candidate in Electrical Engineering and Information Technology at Darmstadt University of Technology, Darmstadt, Germany.
Between 2001 and 2005, he served as a research assistant at national center of excellence in radio communications and power engineering, Tehran Polytechnic. In 2002 and 2005, he was a research engineer at the Iran Telecommunication Research Center (ITRC) and Niroo Research Institute, the leading research organizations of Iran Ministry of Information & Communication Technology and Ministry of Energy, respectively. In late 2005, he joined the Institut für Theorie Elektromagnetischer Felder, Technische Universität Darmstadt. His primary research interest is the application of multiresolution analysis in computational engineering.
Mr. Geranmayeh was the recipient of Deutschen Forschungsgemeinschaft (DFG) graduate research fellowship, the European Microwave Association special travel grant, and the ITRC's grants for both the B.S. and M.S. theses. He was also the second nominee for the EuMC'08 young engineer prizes and the finalist of IEEE/ACES'05 student paper contest. He had an invited talk for Graduiertenkolleg "Physik und Technik von Beschleunigern", in summer 2005.